RSC Advances

ROYAL SOCIETY OF CHEMISTRY

www.rsc.org/advances

Journal Name

RSCPublishing

ARTICLE

Graphitized porous carbon prepared from pyrolysis of sterculia scaphigera and its application in lithium ion batteries

Cite this: DOI: 10.1039/xoxxoooooox

Received ooth January 2015,
Accepted ooth January 2015

DOI: 10.1039/xoxxoooooox

www.rsc.org/

W. X. Wang[a], Y. Wan[a], S. F. Wu[a], M. C. Li[a], L. J. Cao[a], F. C. Lv[a], M. Y. Yang[a], Z. F. Sun[a], R. Sun[b] and Z. G. Lu[a*]

Sterculia scaphigera exhibits exceptional capability to inhale a large amount of water accompanying great volume expansion. In this paper we present, for the first time, the eco-friendly preparation of graphitic porous carbon materials via a simple pyrolysis of H_2O-adsorbed sterculia scaphigera under moderate temperature. Nitrogen adsorption/desorption, X-ray diffraction, Raman spectra and transmission electron microscopy characterizations indicate that the water adsorption plays critical role in developing the abundant micropore architectures and high specific surface area as well as promoting the graphitization degree of the as-obtained porous carbon improved. Furthermore, the as-prepared porous carbon has been demonstrated superior electrochemical performance with a good combination of moderated capacity, good rate capability, extremely stable cycling and high coloumbic efficiency.

1. Introduction

With the depletion of fossil fuel, the exploitation of green and sustainable energy has become increasingly important, which causes the large-scale energy storage devices introducing and developing rapidly [1, 2]. Especially the rechargeable lithium ion batteries (LIB) are one of the most attractive renewable devices because they have successfully driven the wide commercialization of potable electronics and application in electric vehicles areas [3]. However, the development of LIB largely legs behind the progress of consumable electronics and the successful application of LIB in electric vehicles needs further exploration. In particular, the lack of suitable anode material with appropriate comprehensive electrochemical performance is the bottleneck.

In recent years, various nanostructured Si [4], Sn [5], and some types of transition metal oxides [6, 7] with ultra-high theoretical capacities have been utilized as anode materials for LIB owing to their conversion reaction mechanisms for lithium storage. Nevertheless, graphitic carbon, because of its low cost, easy processability, chemical stability, and desirable electrochemical profile [8], has been overwhelmingly used for the anode material of LIB on the market. Inspired by graphite-based carbon, more exploration for novel carbon materials and composites with high capacity or desirable rate performance is underway [8-12]. Soft carbon is a sort of graphitizable carbon, which shows both graphitic and non-graphitic structure [13, 14]. This type of carbon has been of particular interest since its higher capacity over the theoretical capacity of traditional graphite and superior rate capability at high current density [14, 15]. Although several publications about soft carbon derived from petroleum pitch, coke and other organic precursor [14-18] is reported, its electrochemical performance are somewhat undesirable. Moreover, very few literatures investigate the electrochemical properties of soft carbon originated from natural biomass until now.

Herein, we reported a feasible, economic and eco-friendly route to prepare graphitized porous carbon from natural biomass of sterculia scaphigera for the first time. The spindle-shaped sterculia scaphigera is mainly composed of bassorin, galactose and pentaglucose. When it is immersed into water, the natural sterculia scaphigera gradually swells due to the adsorption of large quantity of water. And the swelling sterculia scaphigera recovers to dry appearance after water evaporation. This process involves simple water inhalation and evaporation, eventually leading to the evolvement of highly porous structure. The as-obtained carbons are highly porous possessing good graphitic degree. Most importantly, no metal catalysts were used and the carbonized temperature was moderate (around 800 ^{o}C). Furthermore, no toxic gases were exhausted during the carbonization process. Therefore, this study introduces a green and economic concept, meanwhile provides a feasible approach to prepare graphitized porous carbon materials from natural biomass for application in LIB.

2. Experimental section

2.1 Preparation of graphitic porous carbon

The spindle-shaped sterculia scaphigera (Figure 1a) was first rinsed with deionized water several times to remove the impurity adsorbed on the surface. After that, the whole sterculia scaphigera was soaked in deionized hot-water (approximately 60^{o}) about 5 h so as to inhale enough water. In this process,

water would be smoothly absorbed into the inner of sterculia scaphigera, which triggered volume swelling and development of pore structure, as illustrated in Figure 1c and 1d. When it completely saturates, the sterculia scaphigera inhaled adequate water is dried in oven at 100 °C for 10 h. As shown in Figure 1e, the dried sterculia scaphigeras resembles as a thin film and is highly transparent. Thereafter, the dried products were subsequently annealed at high temperature. Firstly, the temperature was increased from ambient temperature to 250 °C at a heating rate of 1 °C/min and held for 3 h at pure argon (Ar) atmosphere. Secondly, the temperature rose to 850 °C and kept for 6 h (the heating rate is 5 °C/min) in Ar. After cooling to room temperature, the carbonized sterculia scaphigera was finely ground, and then washed with ethanol and distilled water several times to remove the impurity. Finally the sample was dried under vacuum oven at 80 °C for 24 h. The resultant carbon samples derived from carbonized sterculia scaphigera were denoted as SSC-X, where X represents the different carbonization temperature. For the aim of comparison, another carbon was prepared at 800 °C by directly carbonizing natural sterculia scaphigera without adsorbing water and designated as RSSC-800. The whole preparation procedure is schematically illustrated in Figure 1.

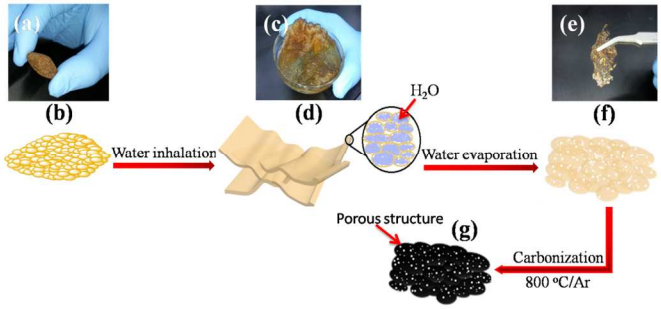

Figure 1. Schematic illustration to prepare carbon materials derived from sterculia scaphigera precursor. (a) sterculia scaphigeras before water inhalation; (b) plenty of water is inhaled into sterculia scaphigera leading to the tremendous volume swelling; (c) the dried sterculia scaphigera after water evaporation at 100 °C for 12 h; (d) carbonized sterculia scaphigera at high temperature.

2.2 Characterizations

The crystallinity of carbonized samples were analyzed by Siemens X-ray generator with Cu kα radiation (λ=0.15406 nm) in the range of 10° to 80°. Nitrogen adsorption/desorption isotherms were measured on a Micromeritics, ASAP2020 gas sorption analyzer at 77 K. All samples were degassed at 200 °C on a vacuum line following a standard protocol before measurement. The specific surface area was determined from N_2 adsorption isotherm by applying Brunauer-Emmett-Teller (BET) theory and the pore size distributions were obtained from the adsorption branch by means of density function theory (DFT). The total pore volumes were determined from the amount adsorbed at high relative pressure of 0.99. Graphitized degree of samples also detected by Raman spectroscopy using Jobin-Yavon T6400 confocal Raman spectrometer with 532 nm diode laser excitation on 1800-line grating. The morphology of samples was characterized with field-emission scanning electron microscopy (FESEM, JEOL 7001F). High-resolution transmission electron microscopy (HRTEM) images were obtained from field-emission transmission electron microscopy (JEOL, JEM-2010F).

2.3 Electrochemical test

For electrochemical measurements, 70wt% active material, 20% acetylene, 10% polyvinylidene difluoride (PVDF) were formulated by adding into N-methyl-2-pyrrolidone (NMP), and ground within agate mortar for 0.5 h to form homogeneous slurry. The slurry was then coated on copper foil uniformly and dried for 24 h at 80 °C in vacuum oven. The loading of active materials was around 1 mg. The electrolyte was composed of a solution of 1M $LiPF_6$ in 1:1 (by volume) ethylene carbonate (EC)/diethylene carbonate (DEC). The sandwich cells were assembled in Ar-filled glove box (Mbraun, H_2O and O_2 < 0.1ppm) by taking the cathode film and Li metal foils acting as anode. Cyclic voltammetry (CV) and impedance experiments were completed using Bio-Logic VMP2 multichannel potentiostat. Electrochemical impedance spectroscopic (EIS) profiles were recorded by applying an oscillating voltage of 5 mV over frequency ranging from 10 mHz to 100kHz. Galvanostatic charge/discharge that primarily tests the cycling life and rate performance under the voltage window 0.05 to 3 V was carried out using Arbin BT2000 multichannel testing equipment at room temperature.

3. Results and discussion

3.1 Structural features of the prepared materials

The structure of resultant sample carbonized with different temperature was analyzed by XRD. A collection of experimental XRD profiles for the four samples is recorded in Figure 2. All carbon samples show the identical patterns, characteristic of 002 major peak at 2θ~27° marked as a typical of graphite like nano-crystallites and broad peak at higher angle 2θ~43° noted by the convolutions of (10) hk bi-dimensional line and the weak 004 reflection [19]. As discussed by Inagaki [20], the appearance of h k lines attributes to turbostratic stacking of hexagonal layers, which reflects the loss of regularity along the c-axis resulting in the formation of disordered carbon material. These XRD patterns match well with the feature of soft carbon material reported in literatures [14, 21]. It is worth noting that the peak (002) slightly sharpens with increasing the carbonization temperature, suggesting that the graphitization degree of as-prepared carbon is gradually enhanced.

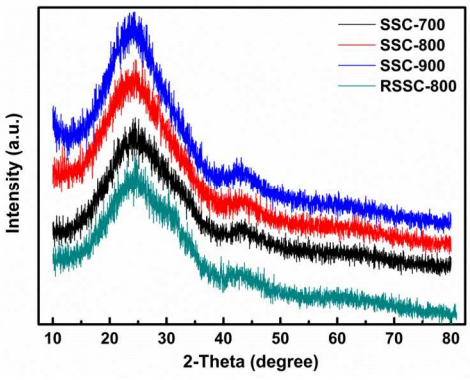

Figure 2. XRD patterns of RSSC-800 and SSC-X carbon specimens.

Further insight into the crystallinity of the carbon structure was investigated by Raman. Figure 3 reveals typical Raman spectra of three carbon samples. These carbon samples exhibit two intense bands marked at 1350 and 1590 cm^{-1}, respectively assigned to the D (disorder carbon) and G (graphite carbon) bands of carbon materials [22-24]. The relative peak height and width of the two carbon bands dramatically vary with the temperature rising from 700 to 900 ^{o}C. Specifically, the G band tends to shift toward higher frequencies and gets narrower when carbonization temperature goes up to 900 ^{o}C, revealing the increasing of interplanar (L_a) and interplanar (L_c) microcrystallite dimension [23, 24]. The ratio of the two band intensity (I_G/I_D) ranges from 0.99 to 1.05 in Figure 3. Interestingly, a broad and weak second-order band was seen at approximately 2700 cm^{-1} for the SSC-800 and SSC-900 samples. For the RSSC-800 sample, the intensity ratio is only 0.93 as shown in Figure S1, and no obvious broad and second-order band emerges around 2700 cm^{-1}. The variation of Raman spectra substantially indicates the increase of graphite degree through water assistant, further supporting the results observed in XRD patterns. In addition, the graphitization degree of SSC-800 has been enhanced as compared with the RSSC-800 sample.

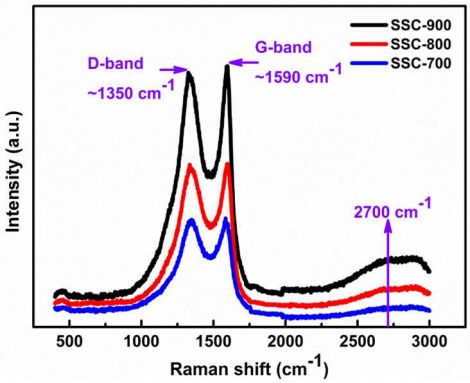

Figure 3. Raman spectra of carbon samples obtained at 700, 800, and 900 ^{o}C.

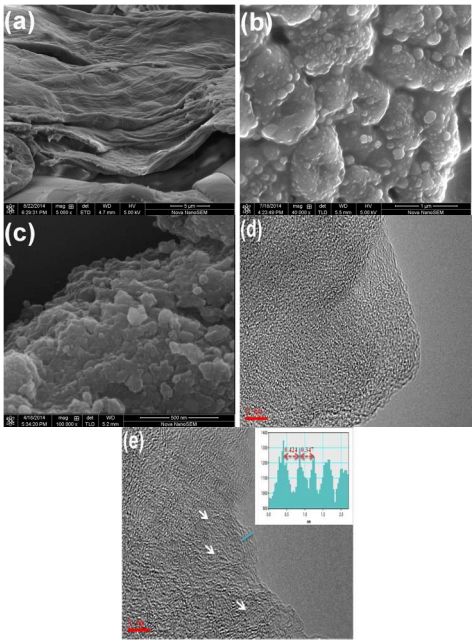

Figure 4. FESEM images of sterculia scaphigera (a) without any treatment; (b) after water evaporation at 100 for 12 h; (c) carbonized at temperature of 800 ^{o}C. HRTEM image of (d) RSSC-800 and (e) SSC-800 carbon material; the inset shows d-spacing of 5 stacking layers of grapheme sheets.

FESEM and TEM technology were applied to characterize the microstructure of synthesized carbon materials. Figure 4a shows the FESEM image of natural sterculia scaphigera without any treatment. It can be seen that the natural sterculia scaphigera mainly comprises smooth and wrinkled sheets with several micrometers. After water adsorption and evaporation, the micromorphology of sterculia scaphigera swells remarkably and evolves into lots of accumulated micro- and nano-particles on the surface of oval bulk. Also the surface looks like rougher than that of raw sterculia scaphigera, as seen from Figure 4b. Meanwhile, the macromorphology of sterculia scaphigera presented in Figure 1e resembles as a transparent thin film. As a result, it can be speculated that the effect of large amounts of water inhalation on the micromorphology is distinctly visible, and the thinner film helps to promote the graphitization of sterculia scaphigera at high temperature. Figure 4c exhibits a high magnification image of carbon sample carbonized at 800 ^{o}C in Ar. It reveals that the bulk sheet-like architecture is constructed by the agglomeration of nanoparticles. Meso/macropore structure also has developed from the accumulated nanoparicles. Figure S2a shows the nitrogen adsorption/desorption isotherms of RSSC-800 and SSC-X carbon materials, while Figure S2b shows the corresponding pore size distribution determined from the adsorption branch using DFT. Compared with the carbon samples derived from sterculia scaphigera without adsorbing water, both the specific surface area and pore size distribution of the SSC-X specimens are quite distinctive. The values of porosity characteristics for all samples are provided in Table S1. The specific area of SSC-700 carbon is as high as 481.74 m^2 g^{-1}, nevertheless the RSSC-800 carbon sample only possesses a specific surface area of 2.19 m^2 g^{-1}. Simultaneously, the microporosity and microporous surface area increase effectively for the SSC-X

specimens. These results synergistically suggest that water inhalation has a considerable improvement on the pore texture of the as-prepared carbon materials.

HRTEM was performed on RSSC-800 and SSC-800 carbon sample to peep at its features in nanometer region, as displayed in Figure 4d and e. No graphene sheets are found stacking along with the 002 plane of carbon in Figure 4d. Interestingly, HRTEM image in Figure 4e indicates the graphitized structure of the obtained SSC-800 carbon material, even though the graphite degree is lower than that of the natural graphite. Furthermore, line profile inserted in Figure 4d quantifies the *d*-spacing of several graphene sheets in the SSC-800 carbon, which can be generally assigned to the 002 plane of graphitic carbon and is in the scope of 0.347~0.424 nm. The graphite crystalline forming the expansion in the *d*-spacing of graphene layers may be in favour of accommodation of extra lithium ions [25]. The micropore textures caused by stacking of tutbostratic disorder structures in Figure 4e also offer additional sites to store more lithium on the pore surfaces [13, 26].

3.2 Electrochemical performance of SSC-X and RSSC-800 specimens

EIS measurement was initially employed to investigate coin cell assembled with carbonized samples. As illustrated in Figure 5a, the EIS consists of a depressed semicircle at the range from high-frequency to middle-frequency and a slopping line at the low frequency region. The intersection of the real axis at the high frequency generally refers to electronic and ionic resistance of the two electrodes and electrolyte/separator (R_{el}). According to the simulated equivalent circuit as shown in Figure S3, the depressed semicircle is actually composed of two overlapped part. The resistance in the high frequency is attributed to SEI film (R_f) and constant phase element (CPE) formed on the surface of two electrode [27-29]. The medium frequency one represents charge-transfer resistance (R_{ct}) and the related double layer capacitance. For the later, CPE is also introduced to precisely simulate the capacitance originated from the surface of active material. The following slope line at low frequency reflects Warburg impedance of lithium ion diffusion [29]. For the series of SSC-X samples, the resistance trend in the high and middle frequency, which is roughly equal to the diameter of the semicircle in the spectra, indicates that lower carbonization temperature gives higher sum of R_f and R_{ct}. Noticeably, the sample RSSC-800 shows the maximum R_{el} and relatively small semicircle. In principle, the variation of graphitization degree, specific surface area and pore structures are primarily responsible for the electrochemical discrepancy of these carbon electrodes. Further electrochemical characterization was performed at a current density of 0.1 C to distinguish specific capacity and cyclability of the three carbon electrodes, as shown in Figure 5b. An obvious feature of Figure 5b is the excellent cyclic performance and reversibility within 100 cycles, although all of these carbon electrodes show large irreversible capacity in the initial cycle. Hence these electrochemical behaviours are basically similar with soft carbon materials reported in literatures [14, 19, 30-32]. Meanwhile, it is obvious that, in the inset of Figure 5b, SSC-800 electrode exhibits a specific capacity up to 423 mAh g^{-1} after 100 cycles and 97% coulombic efficiency, which is comparatively superior to the samples of SSC-700 (364 mAh g^{-1}), SSC-900 (320 mAh g^{-1}) and RSSC-800 (199mAh g^{-1}).

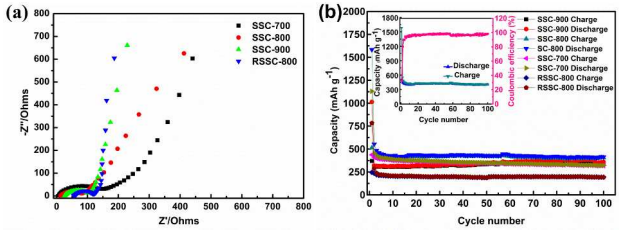

Figure 5. Electrochemically comparative studies of SSC-X and RSSC-800 as anode electrodes versus Li. (a) Nyquist plots of carbon samples before cycling; (b) Cycling performance of different carbon half cells at a current density of 0.1C, the inset is reversible charge/discharge capacity of SSC-800 and the corresponding coulombic efficiency.

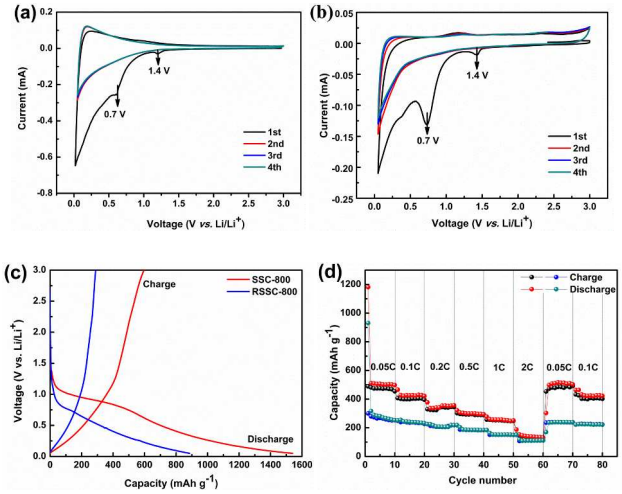

Figure 6. Electrochemical characteristics of RSSC-800and SSC-800 tested in a half-cell. Cyclic voltammograms of (a) RSSC-800 and (b) SSC-800 at a scan rate of 0.1mV s^{-1}; (c) Galvanostatic discharge/charge profiles of the first cycle at a current density of 0.1 C; (d) Rate performance at different current densities from 0.05 to 2 C.

CV curves of RSSC-800 and SSC-800 are depicted in Figure 6a and b at a scan rate of 0.1 mV s^{-1} between 0.05 and 3.0 V. In the first discharge cycle, two distinct reduction peaks around 0.7 and 1.4 V, attributed to the irreversible reactions between carbon electrode and the co-intercalation of solvated lithium ion into graphitized carbon sheets [33-35], are observed for both samples. Another available character in Figure 6a and b is the almost overlapped CV curves in the subsequent cycles, to some extent testifying the stable and superior reversibility. However, the anodic peak at the potential range between 0 and 0.1 V characteristic of graphitic carbon material is nearly negligible for SSC-800 in comparison with sample RSSC-800. It suggests that the electrochemical behaviours are highly dependent on the physical textures. The enlarged specific surface area and developed novel micropore and mesopore from water assisted carbonization of sterculia scaphigeras are favourable for electrochemical activity enhancement. Figure 6c shows the initial galvanostatic charge/discharge profiles of the RSSC-800 and SSC-800 electrode in the range of 0.05 to 3 V. The specific capacity calculated from the first discharge curve reaches up to 1539 mAh g^{-1} for SSC-800 electrode, while the specific capacity of RSSC-800 is only 885 mAh g^{-1}. The corresponding charge capacity of the SSC-800 and RSSC-800

samples is 596 and 289 mAh g^{-1}, respectively. Both electrodes show large irreversible capacity in the initial cycle. The major reasons responsible for that are the formation of SEI film and the decomposition of electrolyte [22] at the voltage plateau of 0.9 V for SSC-800 electrode and 0.7 V for RSSC-800 electrode. The rate performance is shown in Figure 6d. When the current density gradually increased from 0.05 to 0.1, 0.2, 0.5, 1, and 2 C (1 C = 372 mA g^{-1}), the corresponding average discharge capacity decreased from 474 to 400, 340, 290, 253, 130 mAh g^{-1}, respectively. If the current density goes back to 0.05 and 0.1 C again, the average discharge capacity returns to approximately 478 and 402 mAh g^{-1}, respectively. These results indicate good rate capability and a very stable cycling performance. It is worth noting that despite the specific capacity of SSC-800 at rate of 2 C is around 130 mAh g^{-1}, the rate behaviour is superior to the pure graphite electrode [32], and also similar with 30 wt% soft carbon modified hard carbon anodic materials [36]. In addition, although the RSSC-800 sample demonstrated even better rate performance, the reversible discharge capacity of SSC-800 sample is much higher than that of the RSSC-800 sample at the equal current density. The aforementioned results clearly demonstrate that the electrochemical performance of the prepared carbon material is significantly enhanced after water absorption. More possibilities to explain the better electrochemical performance of the SSC-800 electrode is ascribed to the nanoscopic pore structure and graphitized degree synergistically offering a particular route and electric conductivity to enable lithium ion diffusion rapidly. Consequently, the prepared carbon sample SSC-800 may be more suitable to serve as anode material for application in LIB.

4. Conclusions

Sterculia scaphigera was for the first time utilized as a novel carbonaceous precursor to prepare graphitized porous carbon materials. Sterculia scaphigera exhibits tremendous capability to adsorb a large amount of water causing significant volume swelling. On this account, graphitized carbon with favourable micropore architecture can be prepared from carbonization of Sterculia scaphigera at high temperature. It was found that the adsorbed water plays critical role in promoting the graphitization and the formation of highly porous structure. As a result, the obtained carbon materials possessed superior electrochemical performances with high reversible capacity, moderate rate capability and extremely stable cycling properties. Two possible reasons may account for this performance enhancement. On one hand, the carbonized materials have developed abundant micropore structure because water is inhaled into the body of sterculia scaphigera and evaporated subsequently. On the other hand, the graphitization degree of carbonized sterculia scaphigera is effectively enhanced due to the formation of thin film analogues after water adsorption and evaporation. Consequently, the feasible, cost-effective and eco-friendly synthesis route presented in this paper to obtain carbon material brings novel perspectives in fabricating high performance electrode materials for LIB from naturally available biomass.

Acknowledgements

This work was supported by the National Natural Science Foundation of China (21001117), the Starting-Up Funds of South University of Science and Technology of China (SUSTC) through the talent plan of the Shenzhen Government and the Shenzhen Peacock Plan (KQCX20140522150815065). S.Y. thanks the support from the Guangdong and Shenzhen Innovative Research Team Program (No. 2011D052, KYPT20121228160843692).

Notes and references

[a] Department of Material Science and Engineering, South University of Science and Technology of China, Shenzhen, Guangdong 518055, China. E-mail: luzg@sustc.edu.cn

[b] Shenzhen Institutes of Advanced Technology, Chinese Academy of Sciences, Shenzhen, Guangdong 518055, China

Electronic Supplementary Information (ESI) available: [details of any supplementary information available should be included here]. See DOI: 10.1039/b000000x/

1. M. Pasta, C.D. Wessells, R.A. Huggins and Y. Cui, *Nature Communication*, 2012, 3, 1149-1155.
2. B. Dunn, H. Kamath and J.M. Tarascon, *Science*, 2011, 334, 928-935.
3. N.S. Choi, Y. Yao, Y. Cui and J. Cho, *Journal of Materials Chemistry*, 2011, 21, 9825-9840.
4. J. Chang, X. Huang, G. Zhou, S. Cui, P. B. Hallac, J. Jiang, P.T. Hurley and J. Chen, *Advanced Materials*, 2014, 26, 758-764.
5. Z. Zhu, S. Wang, J. Du, Q. Jin, T. Zhang, F. Cheng and J. Chen, *Nano Letters*, 2013, 14, 153-157.
6. L. Hu, P. Zhang, H. Zhong, X. Zheng, N. Yan and Q. Chen, *Chemistry-A European Journal*, 2012, 18, 15049-15056.
7. L. Zhou, H. Xu, H. Zhang, J. Yang, S.B. Hartono, K. Qian, J. Zou and C. Yu, *Chemical Communications*, 2013, 49, 8695-8697.
8. L.W. Ji, Z. Lin, M. Alcoutlabi and X.W. Zhang, *Energy & Environmental Science*, 2011, 4, 2682-2699.
9. A. Vu, Y. Qian and A. Stein, *Advanced Energy Materials*, 2012, 2, 1056-1085.
10. H. Nishihara and T. Kyotani, *Advanced Materials*, 2012, 24, 4473-4498.
11. P. G. Bruce, S. A. Freunberger, L. J. Hardwick and J.M. Tarascon, *Nature Materials*, 2012, 11, 19-29.
12. M. Winter, J.O. Besenhard, M.E. Spahr and P. Novak, *Advanced Materials*, 1998, 10, 725-763.
13. J. Dahn, T. Zheng, Y. Liu and J. Xue, *Science*, 1995, 270, 590-593.
14. F. Bonino, S. Brutti, M. Piana, S. Natale, B. Scrosati, L. Gherghel and K. Müllen, *Electrochimica Acta*, 2006, 51, 3407-3412.
15. M. Schroeder, M. Winter, S. Passerini and A. Balducci, *Journal of Power Sources*, 2013, 238, 388-394.
16. J.E. Chae, K. Annaka, K. Hong, S.I. Lee, H. Munakata, S.S. Kim and K. Kanamura, *Electrochimica Acta*, 2014, 130, 60-65.
17. H. Azuma, H. Imoto, S.I. Yamada and K. Sekai, *Journal of Power Sources*, 1999, 81, 1-7.
18. Y.N. Jo, E.Y. Lee, H.Y. Jeong, Z.H. Lee, K.J. Hong, S.I. Lee and Y.J. Kim, *The Electrochemical Society,* 2012, 1.
19. F. Bonino, S. Brutti, P. Reale, B. Scrosati, L. Gherghel, J. Wu and K. MüLLEN, *Advanced Materials*, 2005, 17, 743-746.
20. M. Inagaki, *New carbons-control of structure and functions*, Elsevier, 2000.
21. J. Gong, H. Wu and Q. Yang, *Carbon*, 1999, 37, 1409-1416.
22. F. Zheng, Y. Yang and Q. Chen, *Nature Communication*, 2014, 5, 1-10.
23. P. Trucano and R. Chen, *Nature*, 1975, 258,136-137.
24. A. Souza Filho, A. Jorio, A. K. Swan, M. Ünlü, B. Goldberg, R. Saito, J. Hafner, C. Lieber, M. Pimenta and G. Dresselhaus, *Physical Review B*, 2002, 65, 085417.
25. E. Yoo, J. Kim, E. Hosono, H.S. Zhou, T. Kudo and I. Honma, *Nano Letters*, 2008, 8, 2277-2282.
26. B.O. Jeong, S.H. Jeong, M.S. Park, S. Kim and Y. Jung, *Journal of Nanoscience and Nanotechnology*, 2014, 14, 7788-7792.
27. J. Zheng, M. Gu, H. Chen, P. Meduri, M.H. Engelhard, J.G. Zhang, J. Liu and J. Xiao, *Journal of Materials Chemistry A*, 2013, 1, 8464-8470.
28. F.Y. Su, C. You, Y.B. He, W. Lv, W. Cui, F. Jin, B. Li, Q.H. Yang and F. Kang, *Journal of Materials Chemistry*, 2010, 20, 9644-9650.
29. V. Freger, *Electrochemistry Communications*, 2005, 7, 957-961.
30. H. Higuchi, K. Uenae and A. Kawakami, *Journal of Power Sources*,

1997, 68, 212-215.
31. T. Iijima, K. Suzuki and Y. Matsuda, *Synthetic Metals*, 1995, 73, 9-20.
32. S.H. Jeong, J.Y. Koh, T.J. Kim and Y. Jung, *Bull. Korean Chem. Soc*, 2014, 35, 2357.
33. Z.J. Fan, J. Yan, T. Wei, G.Q. Ning, L.J. Zhi, J.C. Liu, D.X. Cao, G.L. Wang and F. Wei, *ACS nano*, 2011, 5, 2787-2794.
34. Y.K. Choi, K.I. Chung, W.S. Kim and Y.E. Sung, *Microchemical journal*, 2001, 68, 61-70.
35. Y. Chen, Z. Lu, L. Zhou, Y.W. Mai and H. Huang, *Energy and Environmental Science.*, 2012, 5, 7898-7902.
36. J. Wang, J.L. Liu, Y.G. Wang, C.X. Wang and Y.Y. Xia, *Electrochimica Acta*, 2012, 74, 1-7.

